Preparation and Study Effects of Stirring Time on the Structural and Optical Properties of SnO_2 Nanoparticles

The 5th International scientific Conference on Nanotechnology& Advanced Materials Their Applications (ICNAMA 2015)3-4 Nov, 2015

Dr. Tagreed. M. Al-Saadi
College of Education for Pure Science Ibn-Al-Haithm, University of Baghdad, Baghdad
Email: tagreedmm2000@gmail.com
Dr.Ziyad Tariq Khodair
College of Science, University of Diala.
Noor A. Hameed
College of Education for Pure Science Ibn-Al-Haithm ,University of Baghdad ,Baghdad
Dr. T.A.AL-Dhahir
College of Education for Pure Science Ibn-Al-Haithm ,University of Baghdad ,Baghdad

Abstract

Tin Oxide nanoparticles (SnO_2-NPs) were prepared by mixing ($SnCl_4.5H_2O$) with distilled water at room temperature. The samples were characterized for their crystalline structure, morphology and chemical structure by using X-ray diffraction (XRD), Rietveld refinement, scanning electron microscopy (SEM) and fourier transform infrared spectroscopy (FTIR). The XRD data and Dicvol 91 software analysis the crystal system was found to be tetragonal structure for samples prepared under stirring time for (24,48,72) h with (a=4.745 , c=3.184), (a=4.768 , c=3.255) and (a=4.776 and c=3.257) respectively. The average of crystallite size calculated by using SEM it was 9.45 nm, 14.7 nm and 21.5 nm, for the same times, previously mentioned of stirring. The effect of stirring time on the crystal lattice distortion ratio, specific surface area and dislocation density was discussed. The optical band gap values of SnO_2-NPs were calculated to be about 3.4eV, 3.37eV and 3.2eV under stirring time for 24 h, 48 h and 72 h respectively by optical absorption measurement.

Keywords: SnO_2 nanoparticles, stirring time , XRD ,SEM, Rietveld refinement.

تحضير ودراسة تأثير زمن التحريك على الخصائص التركيبية والبصرية لثنائي أوكسيد القصدير النانوي

الخلاصة

تم تحضيرأوكسيد القصدير (SnO_2) النانوي بخلط ($SnCl_4.5H_2O$) بالماء المقطر بدرجة حرارة الغرفة ولثلاثة أزمان مختلفة من التحريك هي 24 و48 و 72 ساعة. وقد تم تشخيص التركيب البلوري والتركيب الكيميائي وأشكال الحبيبات النانوية المحضرة بإستخدام جهاز حيود الأشعة السينية (XRD) (بالإستعانة بتصفية ريتفيلد، وبرنامج Dicvol 91) والمجهر الإلكتروني (SEM) و(FTIR). تبين ان النظام البلوري هو رباعي, وان (a=4.745 , c=3.184), (a=4.776 and

https://doi.org/10.30684/etj.33.5B.20
2412-0758/University of Technology-Iraq, Baghdad, Iraq

(a=4.768 , c=3.255), (c=3.257 تعود لأزمان24 و48 و72ساعة على التوالي . تم حساب متوسط الحجم الحبيبي

بإستخدام SEM وكان (21.5,14.7,9.45)nm لنفس الازمان المذكورة. كما نوقش تأثير زمن التحريك على نسبة التشوه والمساحة السطحية النوعية ، وكثافة الإنخلاعات للعينات المحضرة . تم دراسة الخواص البصرية وحسبت فجوة الطاقة حيث كانت (3.2,3.37,3.4) eV على التوالي للازمان المذكورة.

الكلمات المفتاحية: ثنائي أوكسيد القصدير النانوي ,زمن التحريك ,SEM,XRD,تصفية ريتفيلد

INTRODUCTION

The semiconductor nano crystals have attracted great interest and focus with respect to their technological applications. The magnetic, optical and electrical properties of such particles were dependent on their particle size [1].

Tin oxide (SnO_2) belongs to tetragonal rutile crystal structure [2]. It has a wide range of applications such as catalysts agent [3], hazardous gas sensors [4], heat reflecting mirrors [5], transparent conducting electrodes for solar cells [6] and optical electronic devices [7]. Different methods are available to prepare SnO_2-NPs such as chemical vapor deposition procedures [8], sol–gel [9], spray pyrolysis [10] and evaporating tin grains in air [11] etc.

In the present work, we prepared tin dioxide nanoparticles using low-cost method and study the effects of stirring time on the Structural and Optical properties of SnO_2-NPs.

Experimental Part : Synthesis and Characterization Techniques

Nanocrystalline SnO_2 powder was prepared by mixing tin (IV) dichloride with distilled water at room temperature:

$$SnCl_4 \cdot 5H_2O(\text{powder}) + H_2O(\text{distilled water}) \longrightarrow SnO_2 + 4HCl + 4H_2O ,$$

Thus 10 g of $SnCl_4.5H_2O$ (Promchimperm Co,98%) was mixed with 800 mL of distilled water. This mixture was maintained under stirring for 24h (sample a) ,48h (sample b) and 72h (sample c). During this period, the solution remained cloudy and white. The pH of the solution decreased rapidly after a few minutes of stirring to reach pH =2 and it remained almost constant. After 24,48 and 72 hours, the stirring was stopped and the mixture was allowed to settle. The gel at the bottom of the beaker was easily separated from the solution by filtering ,it was then washed five times with distilled water and ethanol. After each washing, the mixture was allowed to settle in order to allow the separation of the gel from the solution by decantation .The gel obtained was dried at 80˚C temperature to yield a white powder.

Phase identification determination was carried out using X-ray diffraction (Shimadzu XRD-6000) with Cu $K\alpha_1$ radiation. The average crystallite size (D) of the powder was estimated from the Scherrer formula. XRD data were collected in the 2θ range of (20–70)º using step scan mode with step width of 0.02°. Rietveld analysis was carried out to calculate unit cell parameters. The powder morphology was observed using a (VEGA\\Easy Probe) scanning electron microscope. The chemical groups of the prepared powders were carried out in Shimadzu equipment (IRAffinity-1 FTIR Spectrophotometer).

Results and Discussion

XRD measurement

The XRD pattern of (SnO_2-NPs) is shown in figure (1) as prepared under stirring for 24, 48 and 72 hours. A matching of the observed and standard diffraction angle (2θ) and (d) spacing between crystal planes confirmed that the product is of SnO_2

having a tetragonal structure, which are in good agreement with (JCPDS card no. 41–1445).The observed diffraction peaks correspond to the tetragonal crystalline SnO_2 (rutile) with space groupe ($P4_2/mnm$).The results of diffraction angle (2θ), full width at half maximum (FWHM) β, (d) spacing between crystal planes for three strongest peaks from X-ray powder diffraction are shown in table (1).

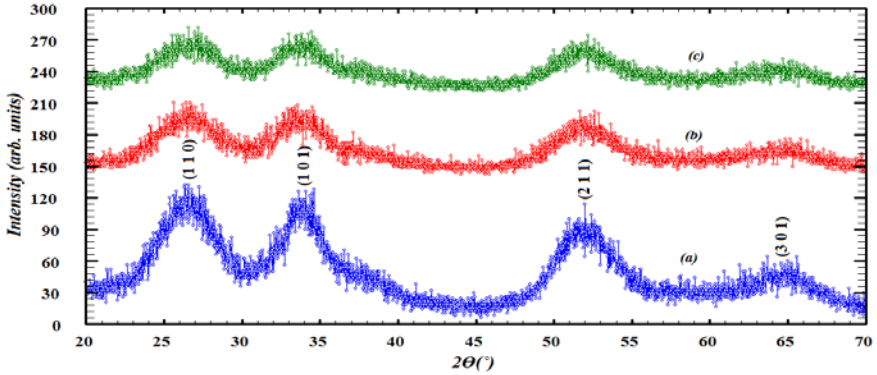

Figure (1) XRD pattern of SnO_2-NPs under different stirring time

Table (1) XRD data of SnO_2-NPs

sample	Stirring time	2θ(°)	d(Å)	β(°)	I/I1
a	24 hr	26.4000	3.37332	0.725958	100
		33.7900	2.65055	2.38000	90
		51.4000	1.77628	2.80000	86
b	48hr	26.6082	3.34739	0.591619	100
		33.3595	2.68377	0.743340	98
		51.7275	1.76580	2.60000	94
c	72hr	27.0675	3.29163	1.06000	100
		33.8556	2.64557	0.31330	97
		51.8240	1.76274	0.24670	93

Crystallite Size Calculation

The average crystallite size was determined by Debye-Scherrer's equation [12-15]:

$$D = \frac{K\lambda}{\beta Cos\theta} \quad \ldots (1)$$

Where:

K: constant$\cong 0.9$, λ: wavelength of Cu $k\alpha_1$ radiation. The average crystallite size for SnO_2-NPs show in table (2).

Table (2) the average crystallite size of SnO_2-NPs.

Sample	stirring time (h)	D (nm)
a	24	8.12
b	48	12.42
c	72	20

From table (2) it shows that the average crystallite size increased as the stirring time increased because of aggregation of particles often took place because of low interfacial surface area with synthesis conditions of the short stirring time [16].

The crystal lattice distortion ratio of SnO_2-NPs at different stirring time calculated by using equation (2)[17]:

$$\beta_{hkl}^2 Cos^2\theta = \frac{4\lambda^2}{\pi^2 D^2} + 32\langle\varepsilon^2\rangle Sin^2\theta \quad \ldots (2)$$

From equations (1&2), it can be deduced the lattice distortion ratio using in the form equation (3):

$$\sqrt{\langle\varepsilon^2\rangle} = \frac{1}{D}\frac{1}{Sin\theta}\frac{\pi}{\lambda}\sqrt{\frac{\pi^2 k^2 - 4}{32}} \quad \ldots (3)$$

Where
$<\varepsilon^2>^{1/2}$ is the crystal lattice distortion ratio, it shows in table (3) of SnO_2-NPs.

Table (3) Crystal lattice distortion ratio of SnO_2-NPs

Sample	stirring time (hr)	D (nm)	$<\varepsilon^2>^{1/2}$
a	24	9.25	0.097
b	48	12.42	0.088
c	72	20	0.032

The crystal lattice distortion ratio decreases with increasing of the average crystallite size because of a decrease in defect concentration by decreasing in the proportion of surface atoms [18].

Specific Surface Area (SSA)

SSA is the area per unit mass, it is factor to determines bulk rates of such reactions (unit m^2/g) [19, 20]. Mathematically, SSA can be determined by use equation (4)[21]. Specific surface area of SnO_2 nanoparticles is shown in table (4).

$$SSA = \frac{6*10^3}{D_p \rho} \quad \ldots (4)$$

Where:
ρ is the density of SnO_2 (6.98 $g.cm^{-3}$).

Table (4) Specific surface area of SnO_2-NPs

Sample	stirring time (hr)	D (nm)	SSA ($m^2. g^{-1}$)
a	24	9.25	92.92
b	48	12.42	69.21
c	72	20	42.97

From table (4) it shows that SSA decreases when the average crystallite size increases because of the degree of agglomeration by the effect of annealing occurring in the material [22].

Rietveld Refinment

Rietveld refinement is a technique used to solve a structure crystalline materials from the powder diffraction data. This method has been so successful that nowadays the structure of materials, in the form of powders, is routinely being determined, nearly as accurately as the results obtained by single crystal diffraction techniques.The results of powder diffraction from X-ray was characterized by reflections (peaks in intensity) at certain positions. The position, height and width for peaks can be used to determine the material's structure. The Rietveld analysis uses a least squares to reduce the difference between the calculated and observed patterns[23–25]. The fitting between observed and calculated diffraction patterns after making crystal structure refinement process of SnO_2-NPs under stirring time for 24 h, 48 h and 72 h are shown in figure (2) and the results of indexing and refinement are shown in table (5). The experimental data are plotted as dots (.) (red line) and theoretical data are shown as solid line (black line). The difference between theoretical and experimental data is shown in the bottom line of each figure (blue line). The vertical lines represent the Bragg's allowed peaks.

Table (5) The results of indexing and refinement for SnO_2-NPs.

Sample	stirring time (hr)	Unit cell parameters (Å)		Crystal System	Space group	Atomic Position			
		a=b	c			atom	x	y	z
a	24	4.7455	3.1847	Tetra.	P $4_2/mnm$	Sn	0.0	0.0	0.0
						O	0.2871	0.2871	0.0
b	48	4.7682	3.2552	Tetra	P $4_2/mnm$	Sn	0.0	0.0	0.0
						O	0.2842	0.2842	0.0
c	72	4.7769	3.2576	Tetra.	P $4_2/mnm$	Sn	0.0	0.0	0.0
						O	0.3146	0.3146	0.0

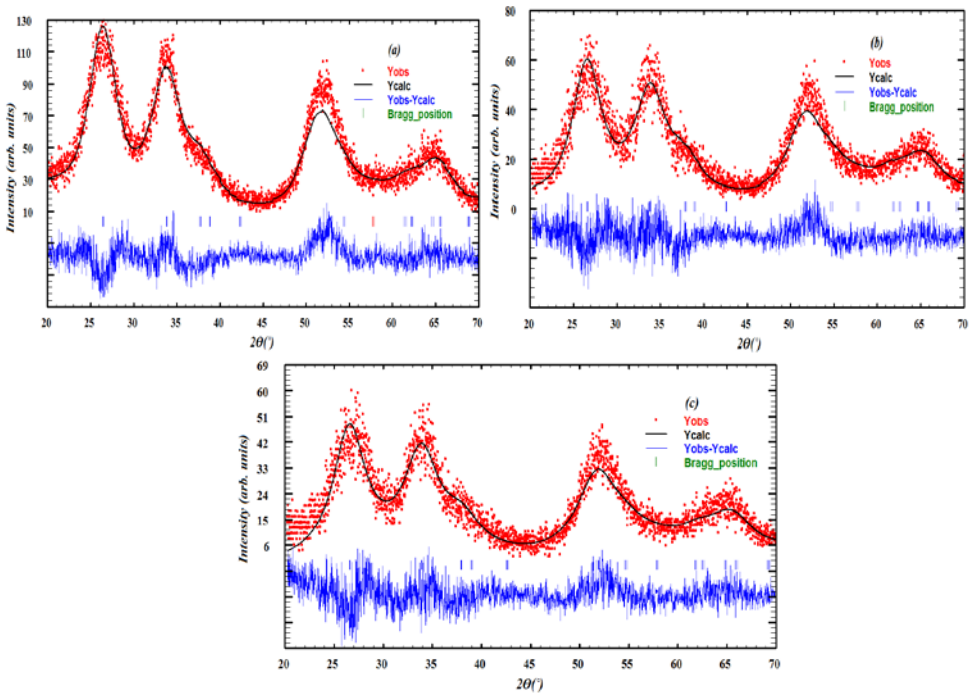

Figure (2) Rietveld refinements of SnO_2-NPs under different stirring time.

Dislocation Density

Dislocation density (δ) is the length of the dislocations present per unit area (lines/m^2). It is an important property for material. Many of the properties of materials are affected by a dislocation, it is a crystallographic defect, or irregularity, within a crystal structure[20, 26]. The dislocation density (δ) in the samples is calculated by using equation (5) [27].

$$\delta = \frac{15\beta Cos\theta}{4\alpha D} \quad \text{... (5)}$$

Where; δ: dislocation density and α: lattice constant (nm).

The number of unit cell Vs dislocation density of SnO_2-NPs for (a, b & c) samples are shown in figure (3).

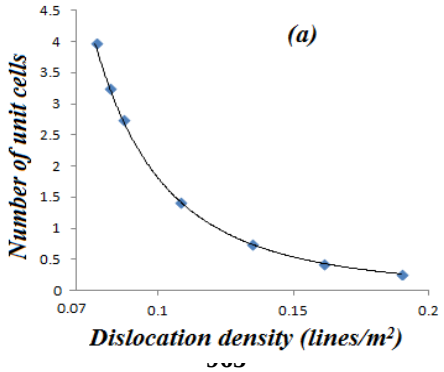

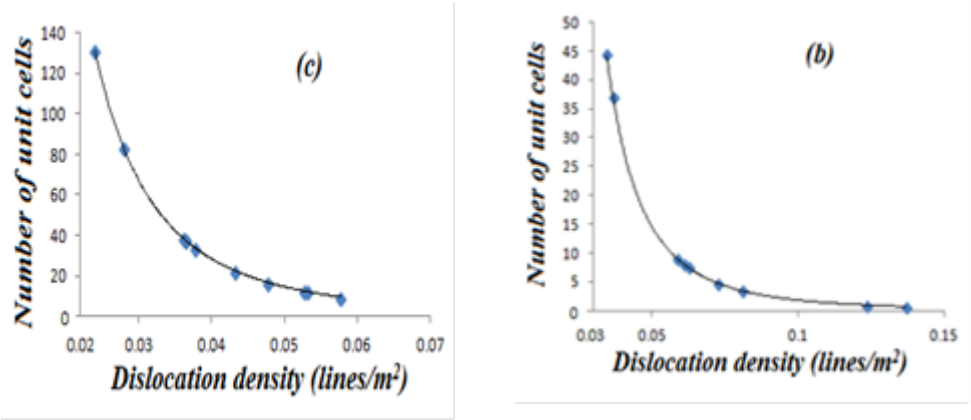

Figure (3) Number of unit cell Vs dislocation density of SnO_2-NPs under different stirring time.

Dislocation density decreases and the number of unit cells increases with increasing in the particle size that leads to increase the crystal growth and decreasing the defects in crystallites this means the crystals with larger dislocation density were harder [28].

SEM images analysis

The SEM micrographs (Fig. 4a) show the particle morphology having homogenous irregular grains, (Fig. 4b) show the particles found to be spherical and there is some agglomeration also observed in image, (Fig. 4c) shows that a network formation and some grains are conglomerated and were grown. It seems clear that the particles size of all samples and agglomeration of particles increase when the stirring time increase. The average crystallite size calculated by using imagej software (Fig.5) and it was found 9.45nm, 14.7nm and 21.5nm under stirring time for 24 h, 48 h and 72 h respectively; this result is consistent with the results obtained from Debye-Scherrer's equation.

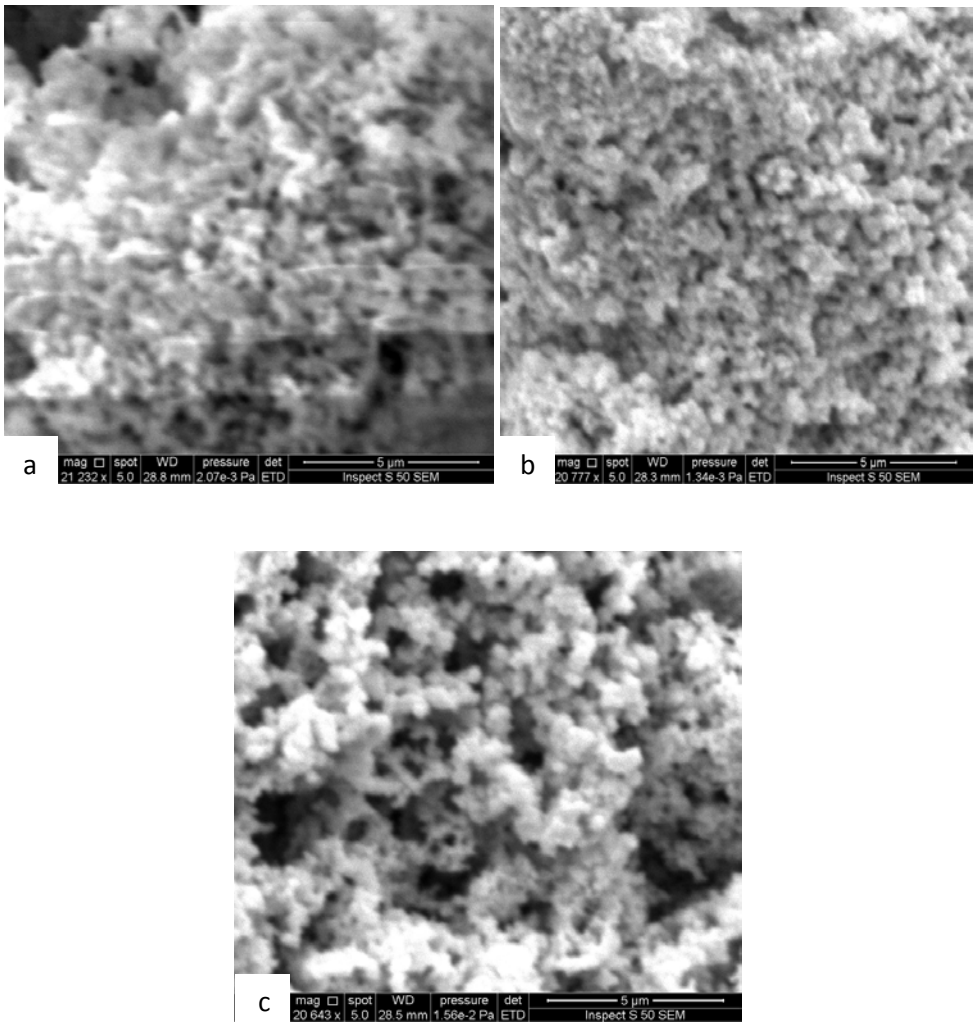

Figure(4) SEM images of SnO_2-NPs under different stirring time.

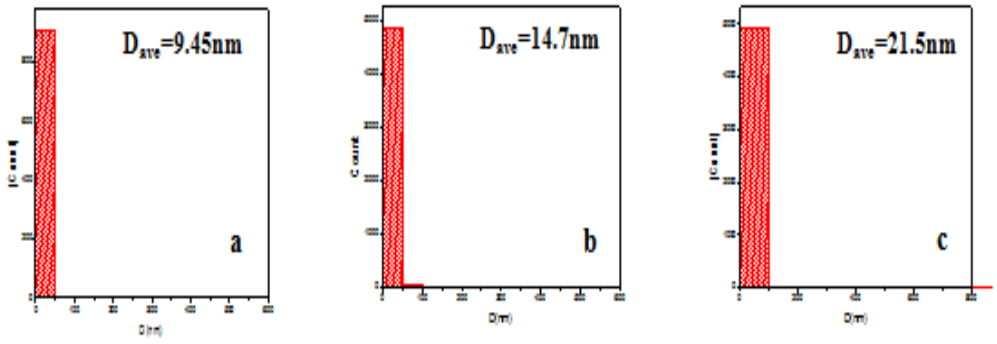

Figure (5) The average crystallite size of SnO_2-NPs under different stirring time

Fourier transforms infrared spectroscopy analysis

Figure (6) show the FTIR spectra of SnO_2-NPs. The analysis was recorded using an FTIR spectrometer in a range between 4000 - 400 cm^{-1}. The shapes of (a, b & c) spectra differ in relation to those recorded for the precipitates produced by hydrolysis of aqueous $SnCl_4$ solutions. SnO_2-NPs showed characteristic FTIR absorption peaks at 677 cm^{-1}, 1232 cm^{-1} and 1633 cm^{-1} which are due to Sn–O vibrational and O–Sn–O stretching modes. The broad bands around 3421 cm^{-1} and the band centered at 2434 cm^{-1} found in the materials are assigned to O–H stretching, which is caused by the vibrations of adsorbed water molecules.

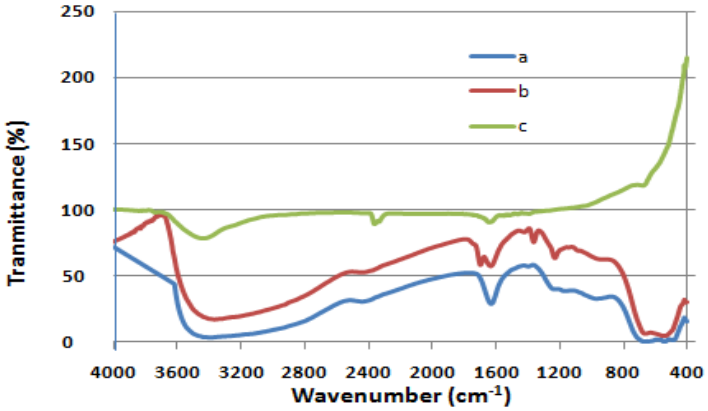

Figure (6) FTIR spectra of SnO_2-NPs under different stirring time.

Optical properties

The absorption spectrum of SnO_2-NPs is shown in figure (7). The figure shows high absorption coefficient in the UV region, whereas it's transparent in the visible region. The edge of absorption got to shorter than wavelength when the time of stirring decreased, and smaller than particles will better absorbed the shorter wavelengths.

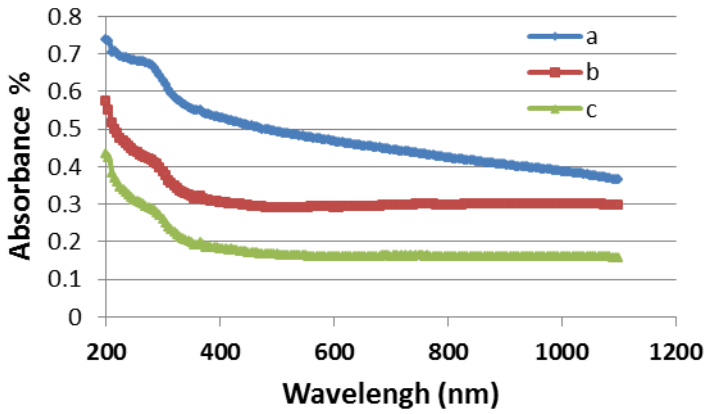

Figure (7) The absorption spectrum of SnO_2-NPs under different stirring time

The optical band gap energy (Eg) of SnO_2-NPs has been evaluated from the absorption spectrum using the Tauc relation [29]:

$$\alpha h\upsilon = A(h\upsilon - E_g)^n \quad \ldots (8)$$

Where:

α: is the linear absorption coefficient of the material, A: is an energy-independent constant, Eg: is the optical band gap, and n: is a constant which determines the type of optical transitions. Figure (8) shows intermediate linear region, the extrapolation of the linear part can be used to calculate the Eg from intersect with hν axis. The values of Eg for SnO_2 are found to be about 3.4eV of sample under stirring time for 24

hours, 3.37eV of sample under stirring time for 48 hours and 3. 2eV of sample under stirring time for 72 hours. The increase in particle size lead to decreasing the energy gap because of the small particles can better absorb shorter wavelengths. The results of band gap change as a function of particle size agreed well with Brus' equation, i.e., the effective mass model (EMM) [30]. This is in full agreement with the analysis of XRD and SEM.

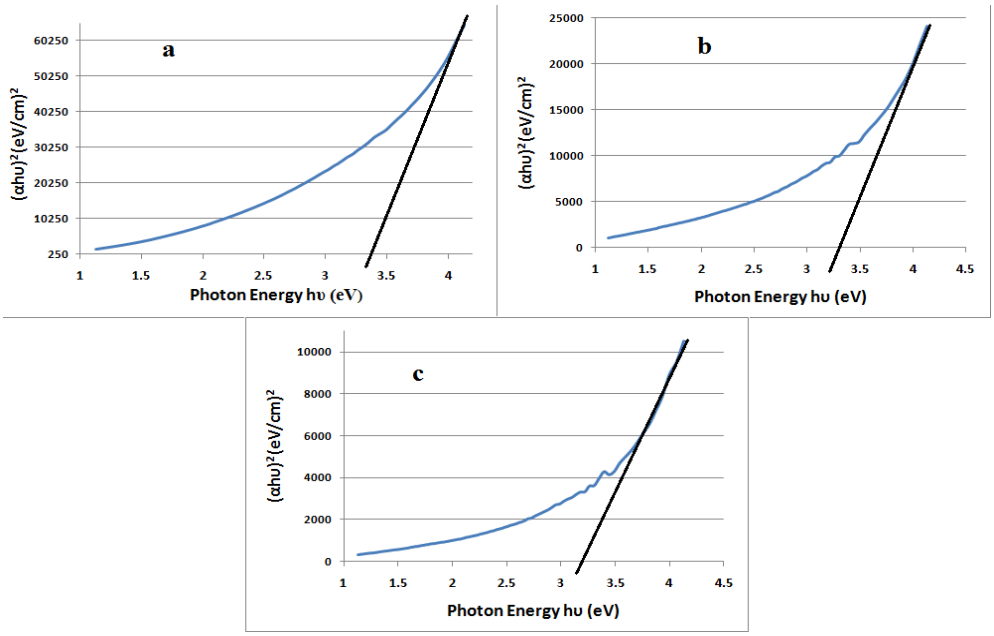

Figure (8) Plot of $(\alpha h\upsilon)^2$ vs. photon energy ($h\upsilon$)of SnO_2-NPs under different stirring time

Conclusions

Tin Oxide nanoparticles (SnO_2-NPs) with a tetragonal structure have been prepared successfully by mixing tin (IV) dichloride with distilled water at room temperature. The SEM micrographs of SnO_2-NPs show that all particles exhibit a spherical shape, the particles size of all samples and agglomeration of particles increase when the stirring time increase. The crystal lattice distortion ratio $<\varepsilon^2>^{1/2}$ and the specific surface area (SSA) are inversely proportional, dislocation density (δ) is indirectly proportional to particle size. A good agreement between XRD data and FTIR data. The smallest optical bandgap of the SnO_2-NPs were found to be about 3.18eV of sample under stirring time for 24 h.

References

[1] R. Bargougui , K. Omri , A. Mhemdi and S. Ammar, "Synthesis and characterization of SnO_2 nanoparticles: Effect of hydrolysis rate on the optical Properties", Adv. Mater. Lett., Vol. 6, pp. 816-819, (2015).

[2] Z. Chen, J. Lai, C. Shek, and H. Chen, "Synthesis and structural characterization of rutile SnO2 nanocrystals", J. Mater. Res., Vol. 18, pp. 1289-1292, (2003).

[3] H. Benhebal and M. Chaib, "Synthesis and characterization pure and alkali catalysts metals-doped tin dioxide", African Journal of Basic and Applied Sciences, Vol. 3, pp.228-234, (2011).

[4] A. Ayeshamariam, V. Vidhya, S. Sivaranjani, M. Bououdina, R. PerumalSamy and M. Jayachandran, "Synthesis and characterizations of SnO_2 nanoparticles", Journal of nanoelectronics and optoelectronics, Vol. 8, pp.1-8, (2013).

[5] A. Ayeshamariam, C. Sanjeeviraja and R. Samy, " Synthesis, structural and optical characterizations of SnO_2 nanoparticles", Journal on Photonics and Spintronics, Vol. 2, pp.4-8, (2013).
[6] G. Li and M. Leung, " Template-free synthesis of hierarchical porous SnO_2", J Sol-Gel Sci Technol, Vol. 3, pp.499-503, (2010).
[7]Y.Wang,I.Ramos and J.J.Santiago-Aviles,"Opticalbandgap and photocond-uctance of electrospun tin oxide nanofibers ",J.Appl.Phys.,Vol. 102, pp.1-5, (2007).
[8] A. Naje, A. Norry and A. Suhail, "Preparation and characterization of SnO_2 nanoparticles", International Journal of Innovative Research in Science, Engineering and Technology, Vol. 2, pp.7068-7072, (2013).
[9] R. R. Kasar, S. R. Gosavi, A. Ghosh, N. G. Deshpande and R. P. Sharma," Influence of Cr doping on structural, morphological and optical properties of SnO_2 thin film prepared by spray pyrolysis technique ", IOSR Journal of Applied Physics, Vol. 7, pp.21-26, (2015).
[10] A.Suhail,A.Naje,G. Muhammed and A. Norry, "Synthesis and characterization of SnO_2 nanoparticles UV-photoconductive detector", International Journal of Current Engineering and Technology, Vol. 4, pp.3610-3613, (2014).
[11] G. Patil,D. Kajale, and G. Jain,"Preparation and characterization of SnO_2 nanoparticles by hydrothermal route",Int. Nano Lett.,Vol.2,pp.46-51, (2012).
[12]V.Mote, Y. Purushotham and B. Dole, "Williamson-Hall analysis in estimation of lattice strain in nanometer-sized ZnO particles", Journal of Theoretical and Applied Physics, Vol. 6, pp.1-8, (2012).
[13] A. Zak, W. Majid , M. Abrishami and R. Yousefi, "X-ray analysis of ZnO nanoparticles by Williamson-Hall and size-strain plot methods", Solid State Sciences, Vol. 13, pp.251-256, (2011).
[14] B. Rehani, P. Joshi, K. Lad and A. Pratap, "Crystallite size estimation of elemental and composite silver nano-powders using XRD principles", Indian Journal of Pure and Applied Physics, Vol.44, pp.157-161, (2006).
[15] Y. T. Prabhu, K. V. Rao, V. S. Sai Kumar and B. S. Kumari, "X-ray analysis of Fe doped ZnO nanoparticles by Williamson-Hall and size-strain plot", International Journal of Engineering and Advanced Technology (IJEAT), Vol. 2,pp.268-274, (2013).
[16]Y. Zhang, J. Zhu, Z. Xu, X. Zhang and Y. Ren, "Effects of synthetic conditions on morphology of hydroxyapatite by chemical precipitation method", Sci-Afric Journal of Scientific Issues, Research and Essays Vol. 2, pp.307-313, (2014).
[17] A. Gaber, M. Abdel- Rahim, A. Abdel-Latief and M. Abdel-Salam, "Influence of calcination temperature on the structure and porosity of nanocrystalline SnO_2 synthesized by a conventional precipitation method", Int. J. Electrochem. Sci., Vol. 9, pp.81-95, (2014).
[18] A. Gaber, M. A. Abdel- Rahim, A. Y. Abdel-Latief, M. N. Abdel-Salam, " Influence of calcination temperature on the structure and porosity of nanocrystalline

SnO_2 synthesized by a conventional precipitation method", Int. J. Electrochem. Sci., 9, pp.81-95, (2014).
[19] M. E. Nielsen and M. R. Fisk, "Data report: specific surface area and physical properties of subsurface basalt samples from the east flank of Juan de Fuca Ridge", Proceedings of the Integrated Ocean Drilling Program,Vol.301,pp.301-205, (2008).

[20] T. Al-Saadi and N. Hameed, "Synthesis and structural characterization of Cr_2O_3 nanoparticles prepared by using $Cr(NO_3)_3.9H_2O$ and triethanolamine under microwave irradiation", Advances in Physics Theories and Applications, Vol. 44, pp.139-148, (2015).
[21] T. Theivasanthi and M. Alagar, "Electrolytic synthesis and characterization of silver nanopowder", Nano Biomed. Eng., Vol. 4, pp.58-65, (2012).
[22] Marco A. da Cunha, Sebastião C. Paolinelli ," Effect of the Annealing Temperature on the Structure and Magnetic Properties of 2% Si Steel", Mat. Res. vol.5 no.3 ,pp.373-378,(2002).
[23] H.M. Rietveld, "Profile refinement method for nuclear and magnetic structures", J. Appl. Cryst., Vol. 2, pp.65-71, (1969).
[24] R. A. Young, "THE RIETVELD METHOD", Oxford University Press INc., New York, (1995).
[25] H. M. Rietveld, "Line profiles of neutron powder-diffraction peaks for structure refinement", Acta Cryst., Vol. 22, pp.151-152, (1967).
[26] K. Kapoor, D. Lahiri, S. V. R. Rao, T. Sanyal and B. PP Kashyap, "X-ray diffraction line profile analysis for defect study in Zr–2.5% Nb material", Bull. Mater. Sci., Vol. 27, pp.59-67, (2004).
[27] V. Jaswal, A. Arora, M. Kinger, V. Gupta and J. Singh, "Synthesis and characterization of chromium oxide nanoparticles", Oriental Journal of Chemistry, Vol. 30, pp.559-566, (2014).
[28] N. Q. Chinh, J. Gubicza and T. G. Langdon, "Characteristics of face-centered cubic metals processed by equal-channel angular pressing", J. Mater. Sci., Vol. 42, pp.1594–1605, (2007).
[29] S. Mehta, S. Kumar, S. Chaudhary and K. Bhasin, "Nucleation and growth of surfactant passivated CdS and HgS NPs: Time dependent Absorption and Luminescence profiles", Nanoscale, Vol. 2, pp.145-152, (2010).
[30] H. Lin, C. P. Huang, W. Li, C. Ni, S. Shah and Y. Tseng, "Size dependency of nanocrystalline TiO_2 on its optical property and photocatalytic reactivity exemplified by 2-chlorophenol", Applied Catalysis B: Environmental, Vol. 68, pp.1-11, (2006).